Proton Transfer in the Copper(II)-Tetrapyridine Catalyzed Oxidation of Acetol (Monohydroxyacetone)

James J. Driscoll and Daniel J. Kosman*

Contribution from the Department of Biochemistry, State University of New York at Buffalo, Buffalo, New York 14214. *Received March 20, 1986*

Abstract: The biomimetic complex copper(II)-tetrapyridine, a nonenzymic analogue of the enzyme galactose oxidase, catalyzes the oxidation of α-keto alcohols by O_2. Classical mechanistic organic protocols have been used to study this reaction by using acetol (monohydroxyacetone) as substrate. Upon the basis of steady-state kinetic studies performed at various oxygen concentrations a kinetic mechanism is proposed in which alcohol substrate binds to catalyst, C; this complex then reacts with oxygen in a kinetically bimolecular reaction yielding catalyst and products. These data can be fit to the rate expression

$$v = k_3[C]\,[O_2]\,[S]/\{(k_2 + k_3[O_2])/k_1 + [S]\}$$

Detailed analysis of the oxygen dependence of the reaction at various pH values yielded the magnitude of rate constants k_1, k_2, and k_3 and their pH dependence. The reaction exhibited an ascending pH-rate profile. In the presence of excess pyridine, the pK_{cs} (equilibrium constant) associated with this pH dependence is 5.51 ± 0.05. In a solvent containing D_2O a shift in this equilibrium (dissociation) constant ($\Delta pK_{cs} = +0.59$) was observed. In addition, there was a kinetic solvent isotope effect (KSIE = 1.15 ± 0.02). A proton inventory was performed indicating that a single hydrogenic site contributed to this KSIE. Additional kinetic experiments were performed examining catalysis by reaction mixtures lacking either excess pyridine, Cu(II), or both excess pyridine and Cu(II). Visual absorbance and ESR spectral studies were performed, examining the state of the Cu(II)-Pyr_4 complex in the presence and absence of excess pyridine at various pH values. The data indicate that Cu(II)-Pyr_4 catalysis of acetol oxidation involves three pH-separable pathways, two of which include concerted catalysis by free (excess) pyridine.

Certain simple transition-metal complexes are capable of serving as effective catalysts for the oxidation of organic alcohol and amine substrates.[1,2] Of particular interest are those reactions which yield the corresponding carbonyl-containing products and either H_2O_2 or H_2O.[3-5] Certain copper complexes are capable of such redox reactions and consequently have been extensively studied.[6] These reactions are not only synthetically useful but some also have potential as model systems for the Cu(II)-containing enzymes galactose oxidase and plasma amine oxidase, which catalyze similar reactions. In addition, metal ion-catalyzed oxidation of cellular reducing equivalents (dihydroascorbic acid, NADH, glutathione) could be related to metal toxicity. Illustrations of this type of physiologic reaction are the oxidation of ascorbate by Cu(II),[7,8] Fe(III),[7,8] and VO^{2+} [9] and of NADH by Cu(II)[10] and VO_4^{3-}.[11] Our interest in such reactions stems from our continuing effort to elucidate the mechanism of action of galactose oxidase, a mononuclear Cu(II) enzyme which catalyzes the two consecutive single-electron transfer reactions involved in the conversion of a primary alcohol and O_2 to the aldehyde and H_2O_2.[12,13]

Table I. Spin Hamiltonian Parameters and Cu(II)/Cu(I) $E^{\circ\prime}$ Values for Galactose Oxidase and Cu(II)-Pyr_4

	galactose oxidase[a]	Cu(II)-Pyr_4
$g_\parallel$	2.227	2.279
$A_\parallel^{Cu}$ (G)	175	191
$A_\parallel^{N}$ (G)	14.5 (2)[b]	11.8 (4)[b]
$g_\perp$	2.051	2.036
$A_\perp^{Cu}$ (G)	0	0
$E^{\circ\prime}$	+300[c,d]	+343[d]

[a] Spin Hamiltonian parameters for galactose oxidase from ref 19. [b] Number of equivalent ^{14}N nuclei, which in galactose oxidase are assigned to imidazole.[19,20] [c] From ref 18 as reported in ref 12. [d] Values vs. NHE in 20% (v/v) DMF, pH = 6.0, 0.02 M Na acetate.

A potential, nonenzymic model system for galactose oxidase is Cu(II)-tetrapyridine (Cu(II)-Pyr_4) which Wiberg and Nigh have shown is reduced readily by α-hydroxyacetophenone in anaerobic reaction mixtures in a strictly second-order reaction.[14] Elements of this anaerobic reaction are comparable to those postulated for galactose oxidase turnover.[12,13] As a nonezymic, biomimetic catalyst, Cu(II)-Pyr_4 can provide new or comparative information regarding Cu(II) active site catalyzed oxidations. Furthermore, Cu(II)-Pyr_4 possesses chemical and structural features quite similar to those of galactose oxidase (cf. Table I). Both Cu(II) sites are axial and square or pseudosquare planar, while the Cu(II)/Cu(I) redox potentials of the two systems are nearly identical. Therefore, to further elucidate the precise role(s) of Cu(II) active sites in the oxidation of primary alcohols and other related substrates, study of this simple catalyst was undertaken.

Experimental Section

Materials. Glass-distilled water was used throughout the experiments. Cu(II)-Pyr_4 was prepared by addition of 16-fold molar excess of pyridine, added with stirring, to stoichiometric amounts of copper perchlorate in a standard buffer solution. This buffer solution was composed of 20 mM sodium acetate (from Baker) in a solvent containing 20% (by volume) DMF. Where indicated, D_2O was substituted for H_2O in the preparation of this mixed solvent. Copper perchlorate was obtained from Alfa Chemical, reagent grade pyridine was obtained from Aldrich Chemical, while DMF was from Fisher Scientific. Solutions were adjusted to the

(1) Benson, D. *Mechanisms of Oxidation by Metal Ions*; Elsevier: New York, 1976; pp 45-66, 83-88.
(2) Nigh, W. G. *Oxidation in Organic Chemistry*; Trahanovsky, W. S., Ed.; Academic Press: New York, 1973; Vol. 3, Part B, pp 1-96.
(3) Adolf, P. K.; Hamilton, G. A. *J. Am. Chem. Soc.* **1971**, *93*, 3420-3427.
(4) Tovrog, B. S.; Diamond, S. E.; Mares, F. *J. Am. Chem. Soc.* **1979**, *101*, 5067-5069.
(5) Tovrog, B. S.; Diamond, S. E.; Mares, F.; Szalkiewicz, A. *J. Am. Chem. Soc.* **1981**, *103*, 3522-3526.
(6) Gampp, H.; Zuberbuhler, A. D. *Metal Ions in Biological Systems*; Sigel, H., Ed.; Marcel Dekker: New York, 1981; Vol. 12, pp 133-189.
(7) Khan, M. M. T.; Martell, A. E. *J. Am. Chem. Soc.* **1967**, *89*, 4176-4185.
(8) Khan, M. M. T.; Martell, A. E. *J. Am. Chem. Soc.* **1967**, *89*, 7104-7111.
(9) Khan, M. M. T.; Martell, A. E. *J. Am. Chem. Soc.* **1968**, *90*, 6011-6017.
(10) Chan, P. C.; Kesner, L. *Biol. Trace Elements Res.* **1980**, *2*, 159-174.
(11) Ramasarma, T.; MacKellar, W. C.; Crane, F. L. *Biochim. Biophys. Acta* **1981**, *646*, 88-98.
(12) Ettinger, M. J.; Kosman, D. J. *Metal Ions in Biology*; Spiro, T., Ed.; Wiley-Interscience: New York, 1981; Vol. III, pp 219-261.
(13) Kosman, D. J. *Copper Proteins and Copper Enzymes*; Lontie, R., Ed.; CRC Press: Boca Raton, FL, 1984; Vol. II, pp 1-26.
(14) Wiberg, K. B; Nigh, W. G. *J. Am. Chem. Soc.* **1965**, *87*, 3849-3855.

0002-7863/87/1509-1765$01.50/0

proper pH with either 1 N NaOH or 1 N $HClO_4$. Electrode response was uneffected by the presence of DMF in the solution. Monohydroxyacetone (acetol) was purchased from Aldrich, redistilled in vacuo prior to use, and stored under N_2. Deuterium oxide (99.8% isotopic purity) was obtained from Sigma. Galactose oxidase was purified from cultures of *D. dendroides* as described.[4,15]

Kinetic Measurements. Initial velocity measurements were made at 25 ± 0.1 °C under air (0.24 mM O_2) except where otherwise noted. A biological oxygen monitor (YSI 53), equipped with a Clark-type electrode, in conjunction with a stripchart recorder was used to record the amount of oxygen uptake upon substrate addition. Velocity was calculated from the tangent to the uptake curve. Each point within a data set was derived from a minimum of three separate runs although data from all runs was used in the computer fitting. The oxygen monitor was calibrated at 20 and 100% O_2. Prepurified oxygen mixtures of 5, 10, and 50% O_2 (in N_2) were obtained from Airco. These mixtures yielded appropriate readings on the oxygen monitor so calibrated.

Data Handling. These initial velocity data were handled by computer fitting to the Michaelis–Menten equation by using the computer program MMFIT (provided by Dr. Eric Dahmer, Department of Biochemistry, State University of New York at Buffalo). Kinetic and pH rate data were then fit to individual rate laws by computer fitting with the program PENNZYME,[16] which optimizes kinetic parameter values through a two-stage nonlinear weighted least-squares minimization. The linear regression analysis program POLYFIT (provided by Dr. James Spain, Department of Biology, Clemson University) was used for fitting intercept and slope replot data and proton inventory data respectively.

ESR and Absorbance Measurements. ESR spectra were obtained at 120 K with a Varian E-9 spectrometer at approximately 9 GHz. Spectra were marked with diphenylpicrylhydrazyl radical (DPPH) as an internal standard; frequency was monitored by using a Hewlett-Packard meter. The field was calibrated by using vanadyl acetylacetonate. Visual absorbance spectra were obtained by using a Perkin-Elmer Model 552A spectrophotometer.

Electrochemical Measurements. Potentiometric determination of $E^{\circ\prime}$ for Cu(II)–Pyr_4 (0.3 mM, 10 mM pyridine) was achieved by using a Princeton Applied Research Model 173 potentiostat/galvanostat with output to a stripchart recorder. A thin cell was used employing carbon and platinum working electrodes, a platinum counter electrode, and a standard calomel reference electrode. Dichlorophenolindophenol (0.3 mM) was used as mediator at pH 6.0 in the NaOAc/DMF-containing buffer used for kinetic measurements. The pulse method of Su and Heineman[17] was employed, converting the net electron flow determined by manual integration of the recorded curves to electron (reduction) equivalents and fitting the data to the Nernst equation, correcting for mediator contributions. The $E^{\circ\prime}$ for the Cu(II)/Cu(I) couple in galactose oxidase has been determined similarly, as well as by reductive titration following the characteristic visible Cu(II) absorbance at 440, 620, and 790 nm. In both of these experiments, Cu(II)–Pyr_4 and enzyme were one-electron acceptors.[12,18]

Results

Physical Chemical Characteristics of Galactose Oxidase and Cu(II)–Pyr_4. To establish Cu(II)–Pyr_4 as a physically reasonable analogue for galactose oxidase, certain relevant physical parameters were determined. The comparative values for these parameters are given in Table I. Both are square-planar Cu(II) sites ($g_x = g_y$) for which ^{14}N shfs (super hyperfine structure) was clearly resolved in the low-field, $M_1 = +^3/_2$ Cu ESR transition in $g_\parallel$: 2N for enzyme,[19,20] 4N for Cu(II)–Pyr_4 (Figure 1). This ^{14}N shfs in the ESR spectra of copper–pyridine solutions was used to monitor the effects of pH and pyridine concentration on the degree of pyridine coordination (vide infra). The splitting in $g_\perp$ in both spectra is due also to ^{14}N shfs, rather than $^{63/65}Cu$ hfs ($A_\perp^{Cu} = 0$, Table I): for Cu(II)–Pyr_4, $A_\perp^N = 12.3$ G; for galactose oxidase, $A_\perp^N = 15.1$ G.[19] Of relevance chemically was that Cu(II)–Pyr_4 exhibited an $E^{\circ\prime}$ for the Cu(II)/Cu(I) couple only slightly higher than that for the enzymic Cu site. Thus, at least the thermodynamic driving force for redox chemistry at these two sites should be comparable.

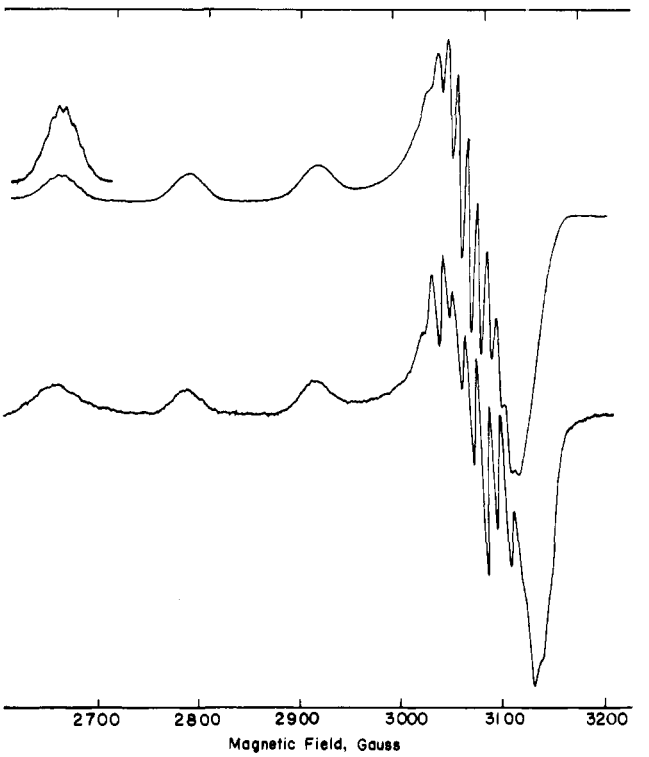

Figure 1. X-band ESR spectra of Cu(II)–Pyr_4 (A) and galactose oxidase (B). Conditions: 0.6 mM galactose oxidase in 0.1 M Na phosphate, pH 7.0, and 5 mM Cu(II)–Pyr_4 in 0.02 M Na acetate, pH 7.0; both solutions were 20% (v/v) in DMF at 120 K. Spectra were recorded at 2 G modulation amplitude and 20 mW microwave power; the signal amplitude was adjusted to scale the spectra. The insert shows the $M_1 = +^3/_2$ transition for Cu(II)–Pyr_4 to illustrate the ^{14}N shfs.

Table II. Dependence of Initial Rate on Complex Concentration[a]

Cu(II)–Pyr_4, mM	velocity, μM/min	
0	0.0 (3.6)[b]	
5.0	16.3 ± 0.4	3.7 ± 0.4 × 10^{-3} min^{-1}[c]
10.0	40.8 ± 1.7	
20.0	79.4 ± 3.8	
40.0	138.7 ± 7.9	

[a] Velocities are the average of triplicate measurements obtained under air at pH 6.0, 25 °C for the oxidation of 490 mM acetol. The reaction mixture contained pyridine at a concentration of 240 mM and Cu(II)–Pyr_4 present at the concentrations indicated. [b] The value 3.6 μM/min represents the blank rate of oxidation catalyzed by pyridine alone present at 240 mM. This value was substracted from all initial velocity measurements. [c] Average value for psuedo-first-order rate constant (±SD) at this concentration of acetol over the concentration range of Cu(II)–Pyr_4 indicated.

Catalysis of Acetol Oxidation by Cu(II)–Pyr_4: Dependence on Catalyst Concentration. Determined by O_2 consumption, the oxidation of acetol (and other α-hydroxy ketones[21]) was catalyzed by Cu(II)–Pyr_4. At an O_2 concentration of 0.24 and 490 mM acetol, the initial velocity of O_2-uptake was determined over the range of Cu(II)–Pyr_4 concentration, 5–40 mM. These data are presented in Table II and show the reaction to be first-order in catalyst.

Oxygen Dependence at Constant pH. These initial velocity data were analyzed in detail. The reciprocal plots of initial velocity data (inverse rate vs. inverse alcohol substrate concentration) obtained at a constant pH and varying, fixed oxygen concentration are displayed in Figure 2C. The plots intersected at a common

(15) Tressel, P. T.; Kosman, D. J. *Anal. Biochem.* **1981**, *105*, 150–153.
(16) Kohn, M. C.; Menten, L.; Garfinkel, D. *Comp. Biomed. Res.* **1979**, *12*, 461–469.
(17) Su, C. H.; Heineman, W. R. *Anal. Chem.* **1981**, *53*, 594–598.
(18) Melnyk, D. Ph.D. Dissertation, State University of New York at Buffalo, 1979.
(19) Bereman, R. D.; Kosman, D. J. *J. Am. Chem. Soc.* **1977**, *99*, 7322–7325.
(20) Kosman, D. J.; Peisach, J.; Mims, W. B. *Biochemistry* **1980**, *19*, 1304–1308.
(21) DaCosta, G. Ph.D. Dissertation, State University of New York at Buffalo, 1982.

Table III. Rate and Kinetic Constants for the Cu(II)–Pyr_4-Catalyzed Oxidation of Acetol

pH	k_1, M^{-1} s^{-1} [a]	k_2, s^{-1} [a]	k_3, M^{-1} s^{-1} [a]	V_{max}, μM/min		K_m, mM	
				calcd[b]	exptl[c]	calcd[d]	exptl[c]
4.0	1.98×10^{-4}	4.89×10^{-5}	7.94×10^{-2}	22.9	25.6	343.2	356.6
5.0	2.50×10^{-4}	6.61×10^{-5}	2.36×10^{-1}	68.0	53.1	491.0	445.6
6.0	6.01×10^{-4}	1.13×10^{-4}	4.80×10^{-1}	138.2	141.2	379.7	412.0
7.0	6.94×10^{-4}	1.49×10^{-4}	6.40×10^{-1}	184.3	163.1	436.0	470.0
8.0	7.90×10^{-4}	1.57×10^{-4}	7.58×10^{-1}	218.2	173.9	428.7	454.0

[a] Rate constants k_1, k_2, and k_3 calculated from individual replots by using the polynomial regression fitting program POLYFIT. [b] Calculated values using k_3 in eq 2 with $[O_2] = 0.24$ mM and $[C_t] = 20$ mM. [c] Experimentally determined at $[O_2] = 0.24$ mM and $[C_t] = 20$ mM. [d] Calculated values using eq 3 with $[O_2] = 0.24$ mM.

point characteristic of an enzymic BiBi sequential kinetic mechanism. The results in Figure 2C also indicated that the system was saturable with respect to alcohol substrate. Figure 2A is an intercept replot of the data at obtained pH 6.0, showing that the system did not reach a limiting velocity at infinite oxygen concentration; therefore, the reaction was not saturable with respect to the second substrate, oxygen. The slope replot in Figure 2B indicates that as oxygen concentration increased the K_m/V_{max} term decreased reaching a limiting value at infinite oxygen concentration. From these data it was concluded that the reaction was first-order with respect to oxygen as shown below

Scheme I

$$C + \text{acetol} \underset{k_2}{\overset{k_1}{\rightleftharpoons}} C\cdot\text{acetol} \xrightarrow{k_3O_2} C + \text{products}$$

This simple mechanism shows that alcohol first binds to catalyst, C; the resulting complex then reacts with oxygen, yielding catalyst and products. From Scheme I, rate eq 1 was derived

$$v = k_3[C]\,[O_2]\,[S]/\{(k_2 + k_3[O_2])/k_1 + [S]\} \quad (1)$$

where

$$V_{max} = k_3[C\cdot\text{acetol}]\,[O_2] \quad (2)$$

when

$$[C\cdot\text{acetol}] = [C_t]$$

and

$$K_m = (k_2 + k_3[O_2])/k_1 \quad (3)$$

pH Dependence of Oxygen Dependence. Similar kinetic analyses were performed at various pH values, thereby determining the pH dependence of the oxygen dependence of the Cu(II)–Pyr_4-catalyzed reaction. Initial velocity data were analyzed by using the computer program MMFIT which fits initial velocity data to the Michaelis–Menten equation and also supplies the kinetic parameters K_m and V_{max}. Following linear regression analysis of these parameters using the computer program POLYFIT, the data obtained at various pH values were then plotted in intercept replot form as shown in Figure 3. When inverse maximal rate at each hydrogen ion concentration was plotted against inverse oxygen concentration, the plots intersected at the origin, with the slope increasing as hydrogen ion concentration increased. The data also indicated that, at all hydrogen ion and oxygen concentrations studied, the system was not saturable with oxygen. These replots, along with slope replots of the same data, allowed direct determination of the individual rate constants, i.e., k_1, k_2, and k_3. Table III lists their response to pH change. From inspection of eq 2, it is seen that V_{max} is directly proportional to k_3; in fact, the data in Table III show that V_{max} rose ninefold while k_3 increased proportionally.[22] These data also show that K_m was independent of pH. Since k_3 also appears in K_m (eq 3), at least one other rate constant must be pH dependent to compensate for the change observed in k_3. As discerned from the individual replots, k_2 (also in the numerator of eq 3) increased by a factor of 3 while rate constant k_1 (a denominator term) increased by a factor of 4. Table III compares experimental and calculated V_{max} and K_m values at various pHs. V_{max} was calculated from eq 2, and K_m was calculated from eq 3, both at an oxygen concentration equal to 0.24 mM.

(22) Of course, k_3 does not change with pH: [C·acetol] in eq 2 does. This term represents the substrate/complex species which reacts with O_2 and which exhibits pH dependent behavior.

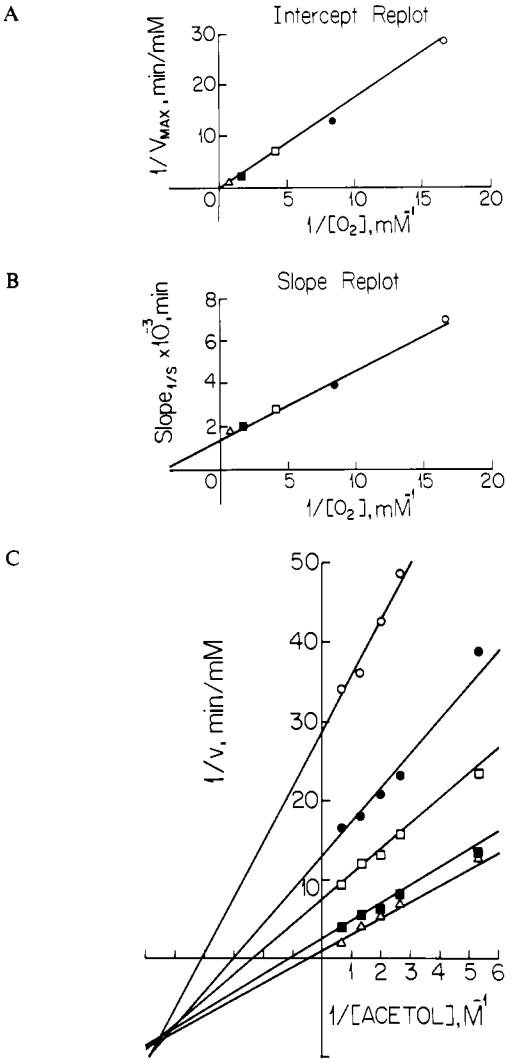

Figure 2. (Part C) Lineweaver–Burk plot for the oxidation of acetol by Cu(II)–Pyr_4 with oxygen as the fixed, varied substrate. At various concentrations, acetol was injected into sealed chambers containing Cu(II)–Pyr_4, and oxygen uptake was monitored. Reactions were performed at pH 6.0, 25.0 °C, under 0.06 (○), 0.12 (●), 0.24 (□), 0.60 (■), and 1.30 (△) mM oxygen. Kinetic constants and plots were determined by computer analysis by using nonweighted linear regression analysis of double-reciprocal plot data. Parts A and B are intercept and slope replots of the data obtained at the various oxygen concentrations used in part C.

Detailed pH Dependence. A detailed analysis of the pH dependence of the Cu(II)–Pyr_4-catalyzed reaction was performed at a single, fixed oxygen concentration (0.24 mM) while varying the concentration of acetol. Again, at each pH value the kinetic parameters K_m and V_{max} were determined by using the computer

Table IV. Kinetic Constants and Parameters for Cu(II)–Pyr_4-Containing Reaction Mixtures[a]

reaction mixture	solvent	V_{max}, μM/min	K_m, mM	β	pK_{cs}	ΔpK_{cs}	KSIE
Cu(II)–Pyr_4 + 240 mM excess pyridine	H_2O	174.0 ± 2.6	382.0 ± 29.0	0.12 ± 0.01	5.51 ± 0.05	+0.59	1.15 ± 0.02
	D_2O	151.0 ± 2.4	328.8 ± 31.0	0.04 ± 0.01	6.10 ± 0.05		
Cu(II)–Pyr_4	H_2O	108.0 ± 3.9	365.1 ± 35.0	(7.5×10^{-4})	5.85 ± 0.05	+0.35	1.08 ± 0.02
	D_2O	101.0 ± 3.4	317.5 ± 34.0	(8.0×10^{-4})	6.20 ± 0.05		

[a] Measurements obtained under air at 25 °C with [Cu(II)–Pyr_4] = 20 mM. Kinetic constants and parameters were determined by using the computer program PENNZYME[16] which yields the standard errors indicated.

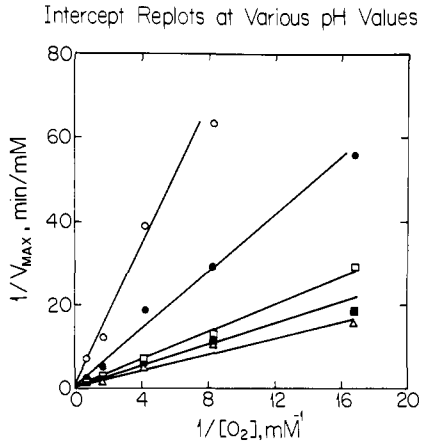

Figure 3. Intercept replots of double-reciprocal data obtained at various pH values with oxygen as the fixed, varied substrate. At various concentrations, acetol was injected into sealed chambers containing Cu(II)–Pyr_4, and oxygen uptake was monitored. Reactions were performed at pH 4.0 (○), 5.0 (●), 6.0 (□), 7.0 (■), and 8.0 (△). Kinetic constants and plots were determined by computer analysis by using nonweighted linear regression analysis of double-reciprocal plot data.

program MMFIT. Figure 4 illustrates that the Cu(II)–Pyr_4 reaction did display a pH dependence, with the reaction velocity increasing as the pH of the reaction mixture increased. By using the kinetic fitting program PENNZYME,[16] regression analysis was performed by fitting the data to eq 4.

$$V_{max_{app}} = V_{max}(1 + \beta[H^+]/K_{cs})/(1 + [H^+]/K_{cs}) \quad (4)$$

The constant K_{cs} is the dissociation constant of a proton from an intermediate involving both catalyst and substrate which appears in the reaction pathway prior to the O_2-dependent step, e.g., the species which appears in eq 2. This fitting routine yielded the following values: pK_{cs} = 5.51 ± 0.05; V_{max} = 174.0 ± 2.6 μM/min; and β = 0.12 ± 0.01. That β > 0 suggested that two catalytically active species were involved in the reaction mechanism under investigation. The identity of these species and their role in the reaction mechanism are considered in the Discussion section. The fit of the data to eq 4 indicated that one of these species supports a residual catalytic activity at low pH values. This activity is associated with the β term which becomes significant only at high hydrogen ion concentrations. A fit of the pH rate data to eq 4 lacking a β term had considerably less statistical significance, with points at pH 4.0 and 4.5 becoming outliers.

Solvent Isotope Study. To further characterize the solvent-dependent protic steps involved in the Cu(II)–Pyr_4-catalyzed reaction, the kinetic solvent isotope effect (KSIE) was determined. The substitution of deuterium for protium can cause effects on specific rate constants of a reaction, thus serving as a useful, nonperturbing probe of a reaction mechanism.[23,24] At various pD, initial velocity studies were performed in the mixed solvent prepared by using D_2O. Maximal velocities were determined at each pD by using MMFIT and then fitting to eq 4 by using PENNZYME. The maximal rate of oxygen uptake in D_2O was 151.0 ± 2.4 μM/min, while the pK_{cs} value determined was 6.10 ± 0.05.

(23) Schowen, K. B.; Schowen, R. L. *Meth. Enzymol.* **1982**, *87*, 551–606.
(24) Schowen, R. L. *Mechanistic Deductions from Solvent Isotope Effects*; Streitweisser, A., Taft, R. W., Eds.; Wiley-Interscience: New York, 1972; Vol. 9, pp 275–332.

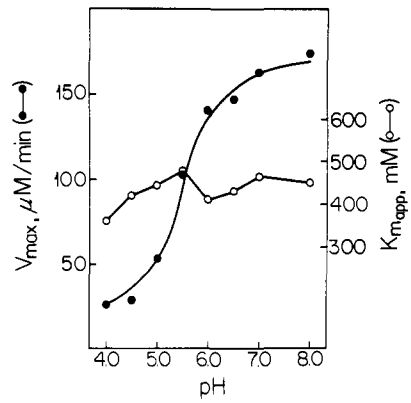

Figure 4. $V_{max_{app}}$ values (●) plotted vs. pH for reactions performed at a constant O_2 concentration of 0.24 mM. The theoretical curve was determined by computer analysis by using eq 2. K_m values (○) are also plotted against pH.

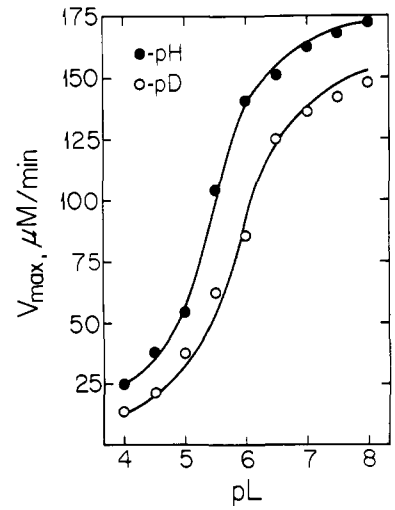

Figure 5. $V_{max_{app}}$ plotted as a function of pL (L = H or D) for the oxidation of acetol at 0.24 mM O_2 catalyzed by Cu(II)–Pyr_4 in the presence of 240 mM excess pyridine. The reaction mixtures included either H_2O (●) or D_2O (○) as solvent. Kinetic constants and best-fitting curves were determined by computer analysis with the program PENNZYME.

Figure 5 compares the rate of reaction in D_2O to that of H_2O. Both rate profiles increased sigmoidally with pL, being statistically well described by eq 4. As the data in Figure 5 indicate, the Cu(II)–Pyr_4-catalyzed reaction did display a KSIE. In addition, with D_2O–DMF as solvent, the pH rate profile displayed a shift in pK_{cs} (ΔpK_{cs} = +0.59) from 5.51 to 6.10. Significantly, when calculated at equivalent pL values above pH 6.0 this KSIE value remained constant. Also, the β term decreased from 0.12 in H_2O to 0.04 in D_2O, indicating that the reaction catalyzed by the second catalytically active species decreased by threefold in a solvent containing D_2O and thus was more sensitive to solvent isotope effects. The kinetic and dissociation constants for the reaction conducted in either solvent are compiled in Table IV. The pH independent K_m value in D_2O compared favorably to that in H_2O, indicating that the apparent Michaelis constant was not altered by the substitution of D_2O for H_2O in the reaction mixture. The insensitivity of the K_m value to D_2O could indicate that rate

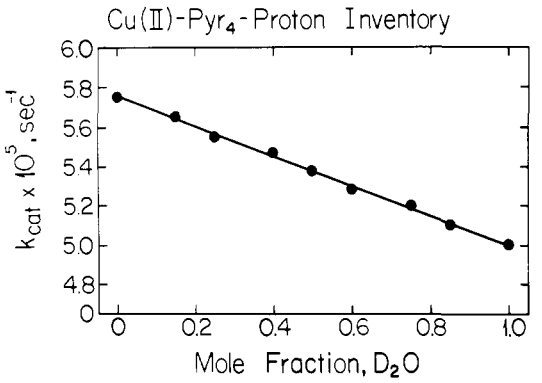

Figure 6. Proton inventory performed at equivalent pL, i.e., corresponding points on the pL-k_{cat} rate profiles (pH 5.51 and pD 6.10). Data points are the average of triplicate measurements while the line is best-fit to a polynomial equation where $n = 1$.

constants k_1 and k_2 were solvent-independent or that k_1 and k_2 exhibited compensating solvent isotope effects as was observed in the pH rate data.

Proton Inventory. To further investigate the KSIE, a proton inventory[23] was performed by using a series of isotopic mixtures of H_2O and D_2O, again prepared in the mixed solvent containing DMF. When comparing rates in isotopic mixtures of water one must use corresponding values on the pL rate profile. Therefore, we chose pH 5.5 and pD 6.1 since these values represent equivalent pL; i.e., these were the respective pK_{cs} values in H_2O and D_2O associated with equal fractions of the catalytically active species associated with K_{cs}. The ratio of $k^{cat}{}_H/k^{cat}{}_D$ was 1.15 ± 0.02. Following linear regression analysis, the data were plotted as k^{cat} vs. mole fraction of deuterium as displayed in Figure 6. The shape of the proton inventory plot was linear ($n = 1$, 99% confidence limit) indicating the existence of a single hydrogenic site responsible for the observed KSIE and, thus, responsible for the slower reaction rate observed in D_2O-containing solvents.[23] This single hydrogenic site presumably was a solvent-derived proton which was involved in (the) rate-determining step(s) of the Cu(II)–Pyr_4-catalyzed reaction. Note that this site need not be the same one(s) associated with the dissociation constant, K_{cs}.

Additional Kinetic Experiments. As shown in Figure 4, a reaction mixture containing 20 mM Cu(II)–Pyr_4, along with 240 mM excess pyridine, displayed a pH rate profile which increased sigmoidally with pH. To further characterize this catalytic mixture, additional kinetic experiments were performed. First, a Cu free reaction mixture containing only pyridine at 240 mM was prepared and used as a catalyst for the oxidation of acetol. The maximal rate of uptake was linear with pH from 5.5 to 10.0 and was small (3.6 μM/min at pH 6.0 and 240 mM pyridine) in contrast to the rate due to Cu(II)–Pyr_4 catalysis (cf. Table II). The same experiment was performed with D_2O as the aqueous component in the mixed solvent system; the maximal rates of uptake were only slightly less than those found with H_2O as solvent. A similar kinetic analysis without any pyridine (or copper) included in the reaction mixture was performed as a control and yielded identical rate constants. Therefore, the oxidation observed in those mixtures lacking Cu(II)–Pyr_4 represented a simple autoxidation of substrate, one which was apparently specific base-catalyzed by hydroxide ion. Thus, pyridine alone was not catalytic, nor was the reaction rate observed with Cu(II)–Pyr_4 attributable to autoxidation. The results also showed that acetate, used to buffer the reaction mixtures, was not catalytic.

A reaction mixture containing Cu(II)–Pyr_4 at 20 mM, but lacking the 240 mM excess pyridine, was characterized also. A pH rate profile of the maximal rate of oxygen uptake at indicated pH values is shown in Figure 7. The pK_{cs} value associated with the ascending pH rate profile observed was 5.85 ± 0.05, while V_{max} was 108.0 ± 3.9 μM/min. These results confirmed that the Cu(II)–Pyr_4 complex, and not the free pyridine, was responsible for the observed oxidation of substrate. However, the maximal rate of uptake was 70% of that found with excess pyridine present.

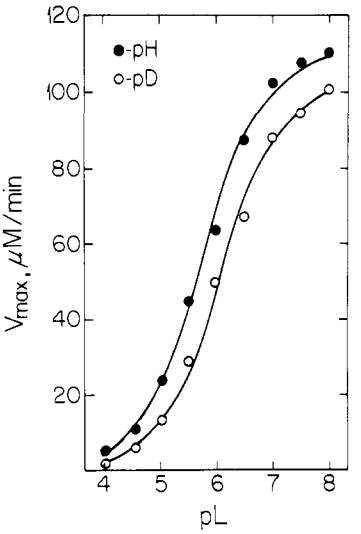

Figure 7. $V_{max_{app}}$ plotted as a function of pL (L = H or D) for the oxidation of acetol at 0.24 mM O_2 catalyzed by Cu(II)–Pyr_4 in the absence of any excess pyridine. The reaction mixture included either H_2O (●) or D_2O (○) as solvent. Kinetic constants and best-fitting curves were determined by computer analysis with the program PENNZME.

The data also were fit to eq 4. Importantly, a β term was not required to achieve a statistically significant fit of the data to eq 4. That is, we did not detect any catalysis by a second catalytically active species ($\beta = 0$). Thus, in the presence of Cu(II)–Pyr_4, pyridine did appear involved in a residual catalytic activity measured at low pH values. With D_2O as solvent for this experiment, a KSIE (1.08 ± 0.02) was measured while a shift in pK_{cs} ($\Delta pK_{cs} = +0.35$) was seen. This shift, from 5.85 to 6.20, was less than that seen Figure 5, i.e., than for the same experiment performed in the presence of excess pyridine. Furthermore, a proton inventory for the reaction catalyzed by complex alone also yielded a value of $n = 1$ for the number of hydrogenic sites.

ESR and Visual Absorbance Spectral Measurements. To elucidate the origin of the group ionization responsible for the apparent pH dependence exhibited in the Cu(II)–Pyr_4 reaction, the Cu(II) metal ion environment was examined at various pH values. ESR spectra of frozen glasses of Cu(II)–Pyr_4, either in the presence or absence of excess pyridine, indicated no detectable change in metal ion coordination occurred between pH 4.5 and 7.5. The spin Hamiltonian parameters (Table I) were invariant over this pH range. At pH values of 4.0 or less an increase was observed in line width indicating the heterogeneity resulting from the dissociation of (a) pyridine ligand(s) from the Cu(II) complex. At pH 2, the spectrum became indistinguishable from that of $Cu(H_2O)_6^{2+}$. This low pH dissociation occurred more readily in the absence of excess pyridine. At pH values of 8.0 or greater aggregation of the Cu species was indicated by a loss of spectral intensity due presumably to the formation of antiferromagnetically coupled bi- and multinuclear Cu^{2+} clusters. Also, scatter was observed in the absorbance spectra at these pH values. Again, these observations were more readily observed in the absence of excess pyridine.

Visual absorbance spectra were obtained of the Cu(II)–Pyr_4 complex both in the absence and presence of excess pyridine, which had no effect on the spectrum. Spectra obtained over the pH range 4.0–8.0 indicated a slight (20%) increase in optical density with pH (data not shown). However, the greatest change in optical density was observed between pH 4.0 and 5.0 (regardless of the presence of excess pyridine) while little change in optical density occurred over the pH range 5.0–7.0, the pH region in which the reaction rate changed. Within this pH region, four pyridine ligands titrated cleanly into $Cu(H_2O)_6^{2+}$ as indicated by the increasing absorbance at 660 nm, the λ_{max} for Cu(II)–Pyr_4 ($\epsilon = 49$ M^{-1} cm^{-1}). There was a distinct isosbestic point at 700 nm upon addition of the fourth equivalent of ligand indicating the conversion of Cu(II)–Pyr_3 to Cu(II)–Pyr_4. The ESR spectrum of the putative

trispyridine species was consistent with the visual absorbance data, i.e, a single set of spin Hamiltonian parameters was resolvable including ^{14}N shfs in the low-field, $M_1 = +^3/_2$ transition. As noted, addition of excess pyridine was without effect on the spectra of Cu(II)–Pyr_4.[25]

Discussion

The kinetic results presented indicate that Cu(II)–Pyr_4 serves as a suitable catalyst for the oxidation of a primary alcohol vicinal to a carbonyl function. Furthermore, the Cu(II)–Pyr_4 reaction displays many of the basic features of the galactose oxidase reaction and should help to better understand the latter. The Cu(II)–Pyr_4 reaction displays a first-order dependence on Cu catalyst concentration indicating the involvement of a single Cu(II) site at or prior to the rate-determining step. This does not discount the possibility of another Cu(II) interacting later in the reaction mechanism. For example, although the anaerobic reduction of Cu(II)–Pyr_4 by ketol was kinetically first-order in complex, obviously two Cu(II) atoms were required for the oxidation of each ketol to ketoaldehyde product.[14] The Cu(II)–Pyr_4 reaction also displays Michaelis–Menten kinetics with respect to [acetol] and, thus, involves kinetic formation of a Cu(II)–Pyr_4·acetol complex, not unlike those complexes described by Benson in his discussion of metal-ion-catalyzed oxidation of primary and secondary alcohols.[1] As the kinetic data illustrate, the Cu(II) complex studied here is capable of catalyzing a bisubstrate process in which alcohol substrate binds first, similar to the ordered BiBi sequential kinetic mechanism followed by galactose oxidase.[26] These similarities demonstrate that simple mononuclear Cu(II) complexes can be useful in understanding the role of such prosthetic groups in metalloenzyme-catalyzed redox reactions.

Kinetic and Spectral Observations. Certain complexities exist in the mechanism of the Cu(II)–Pyr_4 reaction, as do differences from the galactose oxidase one. One puzzling feature of the Cu(II)–Pyr_4 reaction is the pH dependence observed in the absence and presence of excess pyridine. The apparent pK_{cs} value of the group(s) responsible for this ionization differs in these reaction mixtures, being 5.51 with excess pyridine present and 5.85 without. The results indicate that the group responsible for this pH dependence is not free pyridine, since similar sigmoidal pH rate profiles are seen both in the absence and presence of excess pyridine. In addition, ESR data show that dissociation of an equatorially bound pyridine ligand from the complex does not occur in the pH region 4.5–7.5. Lastly, the apparently linear dependence of autoxidation rate on pH indicates that free acetol ionization does not underlie the pH dependent kinetic behavior, as is true for the spontaneous oxidation of ascorbic acid, for example.[7] These kinetic and spectral observations exclude obvious possible group(s) responsible for this pH dependence. Potentially, the observed ionization represents proton dissociation from a reaction intermediate which occurs subsequent to acetol interaction with the Cu(II)–Pyr_4. Indeed, the pH dependent rate data do fit to an eq 4 describing a prototropic event which follows substrate–catalyst complexation.[27]

A second catalytically active species is detected at low pH in the presence of excess pyridine. The results indicate that the β term used in eq 4 to describe this catalytic activity is negligible when excess pyridine is omitted from the reaction mixture or when the reaction is studied at neutral pH. This result suggests the involvement of free pyridine, existing as pyridinium, in the less productive pathway. Nonetheless, the data indicate that a concerted catalytic mechanism does obtain at neutral pH since the sum of the pH independent V_{max} values for catalysis by pyridine alone (4.8 μM/min) and by Cu(II)–Pyr_4 alone (108.0 μM/min) is less than the value determined when the two are simultaneously present (174.0 μM/min). This enhancement cannot be due to a simple ionic strength effect since measured velocities were uneffected by $NaNO_3$ up to 2 M (data not shown).

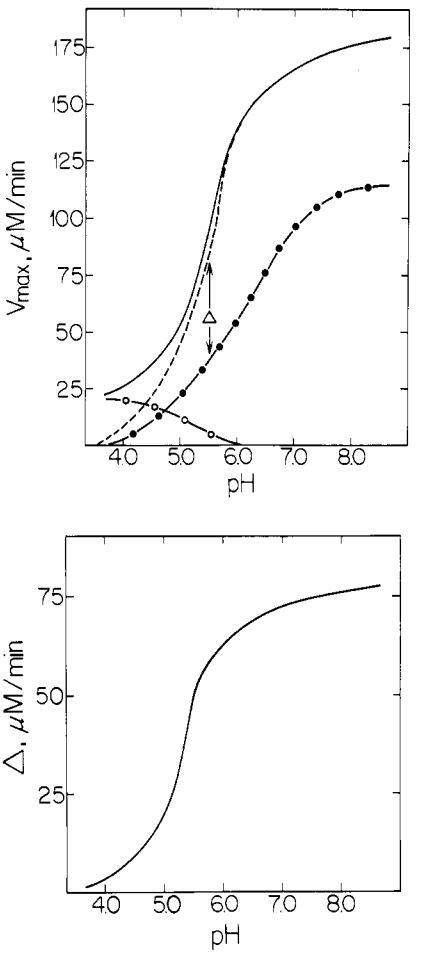

Figure 8. (A) V_{max} plotted as a function of pH for the oxidation of acetol catalyzed by Cu(II)–Pyr_4. Simulated lines are shown for this reaction in both the presence (—) and absence (-●-●-) of excess pyridine. The contribution of a $pyrH^+$ dependent reaction was subtracted from the data obtained in the presence of excess pyridine and is represented by (-o-o-). The difference between the corrected rates (- - -) and the rates found in the absence of excess pyridine is also shown (Δ). (B) shows the pH dependence of this difference, Δ.

Reaction Pathways. The simplest rationalization of this kinetic behavior is that at neutral pH a minimum of two pathways could be contributing to catalysis, one involving concerted catalysis by complex and pyridine (presumably functioning as a general base), the other involving only complex. The former pathway makes a contribution sufficient to enhance the turnover rate overall. Kinetically, it must be more efficient, but without a priori knowledge of the partitioning of the reactants between these two putative pathways, the inherent activities of each cannot be determined. Indeed, in the presence of excess pyridine, only the concerted scheme may obtain. At pH 4 (or below), these two pathways do not contribute to catalysis. That is, for complex alone, $\beta = 0$, and, in addition, pyridine is present at this pH as pyridinium so it could not be providing concerted, general base catalysis. An alternative third mechanism is one in which the pyridinium ion acts as a general acid catalyst and in this way is a component in

(25) The stability constant for Cu(II)–Pyr_4 in 0.5 M $NaNO_3$ is 3.5×10^6 M [Sillen, L. G.; Martell, A. E. *Stability Constants of Metal Ion Complexes*; Chem. Soc. Special Publ.: 1964; no. 17.] with $K_4 = 7$ M^{-1}. These spectral titrations indicate that in the medium used herein the latter value is appreciably larger. The homogeneity of the Cu(II) species in solution under all conditions is indicated by these spectral data as well as by the well-behaved electrochemical and pH dependent kinetic data, both of which would reflect additional equilibria (e.g., changing populations of multiple Cu(II) complexes).

(26) Kwiatkowski, L. D.; Adelman, M.; Pennelly, R.; Kosman, D. J. *J. Inorg. Chem.* **1981**, *14*, 209–222.

(27) The fit to eq 4 does not define K_{cs} as a microscopic constant; K_{cs} may well represent group ionization associated with a number of discrete intermediates. Although the proton inventory suggests that a single hydrogenic site is involved in the reaction step(s) probed by the KSIE, as noted in the text, pK_{cs} may be associated with a distinct ionization site. This site could, in effect, be associated with interconvertible catalyst and acetol complexes. These could involve ligand (pyridine) dissociation. We have no experimental evidence that addresses this question explicitly.

the low pH, residual catalytic activity which, while observed only in the presence of excess pyridine, is Cu(II)–Pyr_4 dependent as well. Interestingly, this low pH pathway exhibits a relatively large KSIE (2.8) which might be expected of a (partially) rate-limiting proton transfer from the pyridinium ion.

If this analysis is correct, then the pH rate profile for the reaction with excess pyridine contains a descending component as pH increases due to the conversion of pyridinium to pyridine and an ascending one due to the increasing free pyridine in the conjugate base form. The former can be simulated assuming a pH residual V_{max} ($pyrH^+$) = V_{max} and pK_a = 4.9 for pyridine using eq 5. The contribution of this pyridinium-dependent reaction

$$V_{max_{app}}{}^{pyrH^+} = V_{max}{}^{pyrH^+}/(1 + H^+/K_a{}^{pyrH^+}) \qquad (5)$$

at a given pH can be subtracted from the data obtained in the presence of excess pyridine; this is illustrated in Figure 8. The difference, Δ, between this corrected pH rate profile and that obtained in the absence of excess pyridine could be due to the concerted catalysis due to free pyridine. If plotted vs. pH, therefore, Δ should increase as $pyrH^+ \rightarrow pyr + H^+$. This plot is presented in Figure 8B. The fit of these data to the standard function (cf. eq 4, $\beta = 0$) yields as pK_a = 5.0, reasonably close to that of pyridine determined in the same solvent (4.9). What this analysis also shows is that the "shift" in pK_{cs} associated with excess pyridine noted in the experimental curves (5.85–5.51) is a consequence of the additive effect of multiple overlapping pH dependent processes.

Proton Dependent Events. This descriptive model of Cu(II)–Pyr_4 catalysis can be discussed further with reference to the KSIE and proton inventory results. Free pyridine did cause a change in the KSIE, although leaving the proton inventory uneffected. The KSIE was not large in either case, 1.08–1.15. These values contrast with those for the lipoprotein lipase reaction (KSIE = +1.97),[28] for example, in which a solvent-derived proton is intuitively involved in the rate-determining step. Significantly, the KSIE observed here was pH independent above pH 6.0. If the KSIE originated from the group ionization detected in the pH V_{max} profile (pK_{cs} = 5.5), the isotope effect should have become negligible as this group completely titrated. That is, as the fraction of solvent exchangeable bound sites became diminishingly small, so would the occupancy difference between protium and deuterium. Such a decrease in the KSIE was not observed. One explanation for this behavior is that the isotope effect originated from the transfer of a water proton. Substitution of D_2O for H_2O as proton donor would yield a KSIE which effectively would be constant within the pH range employed in these experiments.

The origin of this dissociation, pK_{cs} = 5.5, can be inferred from the value, ΔpK_{cs} = +0.59 pH units (excess pyridine). This shift and the corresponding reactant state fractionation factor which can be calculated by using this value, ϕ^{RS} = 0.74, are like those characteristic of proton ionizations from a heteroatom, i.e., O, N, or S and, as discussed below, with our proposed mechanism and possible identification of the group responsible for the apparent ionization.

Metal–Substrate Complex Formation. Previous studies of metal-ion-catalyzed oxidation of ketoalcohols have shown that enolization of the ketol substrate may occur, allowing formation of a copper chelate involving the enolate anion.[3,14] The enolization reactions themselves have been attributed to catalysis by the metal ion.[3,14] Similar complexation of Cu(II) by a phenol[29] or of Cu(II),[7,8] Fe(III),[7,8] or VO^{2+} [9] by dihydroascorbate, prior to metal-catalyzed electron transfer from substrate to O_2, has been proposed also. In these examples, too, the metal was thought to facilitate enol (phenol) ionization concommitant with formation of the metal–substrate complex. The first-order dependence on Cu complex concentration observed for the reaction studied here is consistent with Cu(II)-catalyzed enolization of the ketoalcohol substrate followed by complexation of the Cu(II) as described below.

Scheme II

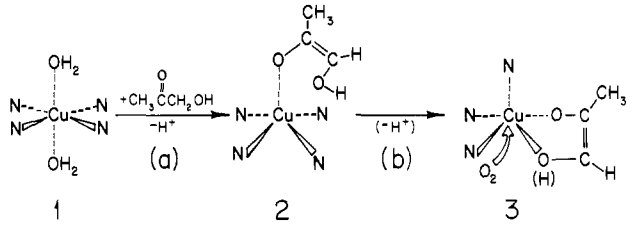

The formation of a metal–ketol chelate would promote the ionization of the hydroxyl proton. As noted, the observed shift in pK_{cs} value is consistent with the ionization of a proton from a heteroatom, that is, its magnitude falls within the range expected for proton dissociation from a hydroxyl group.[23]

Reaction Mechanism. Any reaction mechanism proposed for the Cu(II)–Pyr_4 catalyzed oxidation of acetol must be in accord with certain experimental observations or reasonable inferences based on these results. These are (1) complex formation between the metal-ion and the ketoalcohol substrate; (2) the inclusion of a prototropic event occurring subsequent to metal–ketol complexation; (3) the kinetic formation of a ternary complex requiring participation of the metal–ketol complex and O_2; and (4) the direct involvement of the O_2 in the redox process, presumably functioning as acceptor in the two, one-electron transfers from the substrate. One such scheme consistent with these features is discussed below.

Copper(II)–Ketol Complex Formation. The formation of the putative copper(II)–ketol complex is illustrated in Scheme II. In step (a), metal-ion-catalyzed enolization of acetol involves the displacement of an axial H_2O by the carbonyl oxygen. This reaction leads to the conversion of the D_{4h} Cu(II)–Pyr_4 complex to the square pyramidal enolate one, **2**, which has approximate C_{4v} symmetry. Step (b)—the formation of an enolate–alcohol chelate—involves a realignment of the principal coordinate axes of the Cu(II) atom, i.e., a virtual displacement of an equatorial pyridine by the alkoxide anion. This may or may not involve the loss of the alkoxy proton. The resulting complex, **3**, could be either square pyramidal as illustrated or octahedral with both rhombic and tetragonal distortion. The π-bonding character of the enolate would promote the formation of square pyramidal complex **2**, while the chelate effect would stabilize complex **3**.[30] Note, however, that this scheme is speculative: no explicit (spectral) evidence exists which could be used in support of this model. The axial coordination of alcohol substrate to the Cu(II) in galactose oxidase has been suggested, however, based on a variety of spectral and kinetic measurements.[12,13] Furthermore, octahedral Cu(II), e.g., copper(II)–trisbipyridyl, is not reactive with α-ketoalcohols.[14] Thus, an initial axial (H_2O) site appears to be a requisite structural feature for catalysis. Note that in complex **3**, acetol is formally represented by an electronic analogue of the catechol and dihydroascorbate (mono) dianions, reasonably thought to be intermediates in the oxidation (by O_2) of the corresponding diols.[7-9] Indeed, a complex like that illustrated by structure **3** has been suggested as intermediate in the latter reactions.[7,8]

Catalysis of H^+ Ionizations. As noted above, the proton ionization in step (a) is postulated to be metal ion catalyzed. Comparisons of rates of enolization vs. oxidation in systems like this one indicate the quantitative dominance of metal-ion- over base-catalyzed enolization.[3,14] Such a metal-ion-catalyzed ionization would occur prior to or coincident with complex formation and, thus, lead to an "activated" metal–ketol complex, satisfying requirement 2.

The C–H hydrogenic site does not readily exchange with D_2O, and, thus, would not yield a KSIE. However, enolization of the acetol substrate yields a Cu complex with potential as the intermediate responsible for the kinetically detected ionization, satisfying requirement 2 above. Thus, the excess pyridine could act at step (b) to facilitate removal of the hydroxyl proton. Viewed either as a metal-coordinated saturated alcohol (pK_a = 7–10)[23]

(28) Quinn, D. M. *Biochemistry* **1985**, *24*, 3144–3149.
(29) Kushioka, K. *J. Org. Chem.* **1984**, *49*, 4456–4459.
(30) Hathaway, B. J.; Billings, D. E. *Coord. Chem. Rev.* **1970**, *5*, 143–207.

or an analogue of an enediol-like species, e.g., dihydroascorbic acid (pK_a = 4.0), this group could exhibit a kinetic pK_{cs} of 5.8.[27]

Molecular Oxygen Participation. Similar to the galactose oxidase reaction,[26] the Cu(II)–Pyr_4-catalyzed oxidation also is strictly first order with respect to [O_2]. The kinetic results indicate formation of a ternary complex involving O_2 interacting with the copper(II)–ketol complex (Scheme I). The same dependence on [O_2] has been observed by Barron,[31] Weissberger,[32] and Khan and Martell[7] in analogous studies of metal-ion-catalyzed oxidation of various organic substrates. Furthermore, the formation of a ternary metal–substrate–oxygen complex has been precedented in the literature by George et al.[33] by using a ferrous complex and by Beck and Gorog[34] in a study of the oxidation of ascorbic acid by cobalt(II)–glycylglycine.

The formation of the enolate/alkoxide–copper(II) complex would facilitate the required, subsequent two, one-electron transfers from substrate to O_2 expected for the overall catalytic reaction. Khan and Martell[7,8] presented evidence for formation of a metal–ascorbate complex analogous to **3** above (Scheme II), formed in a preequilibrium step, followed by a rate-determining one-electron oxidation of the (metal-complexed) ascorbate monoanion by O_2. As illustrated in Scheme II, electron transfer to O_2 was postulated to be via the open axial coordination site. A similar direct participation by the metal–chelate in the electron transfer is presumed for the Cu(II)–Pyr_4 reaction.

Although the prototropic events investigated in some detail here do not explicitly bear on these electron transfers—nor on possible reaction intermediates associated with the first of these transfers—two experiments were performed (data not shown) which do. An initial, single-electron transfer to O_2 would generate O_2^-; thus, superoxide dismutase might be expected to affect the rate of the turnover of substrate. In fact, addition of this enzyme to reaction mixtures was without effect on the rate of O_2 consumption. Also, catalytic turnover of substrate could involve cycling of Cu(II)/Cu(I), e.g., in the presence of O_2, the reduction of complex by ketol (as described by Wiberg and Nigh)[14] could be followed by simple, O_2-dependent reoxidation of Cu(I)–Pyr_4 (the k_3 step in Scheme I). Reoxidation of Cu(I)–Pyr_4 (prereduced by anaerobic acetol or dithionite) by O_2 was, indeed, rapid (k_0 = 2.5 × 10^3 M^{-1} s^{-1}, cf. k_3 in Table III) and, thus, could be kinetically competent in turnover. However, anaerobic reduction of complex by acetol was not k_r = 2.8 × 10^{-4} M^{-1} s^{-1} at pH = 6.0 (cf. k_1 = 6.01 × 10^{-4} M^{-1} s^{-1} at the same pH, Table III). These comparisons indicate that turnover did not involve copper complex reduction/reoxidation. This appears true for VO_2^+-catalyzed oxidation of ascorbate as well.[9] Indeed, the kinetically sequential nature of the reaction (cf. Figure 2C) requires that O_2 react with catalyst prior to release of product and with a Michaelis complex (or intermediate) which is reversibly linked to the initial alcohol substrate–catalyst one. This requirement would appear to exclude a mechanism which kinetically separates ketol (reduction) and O_2 (reoxidation).

On the basis of the results and analysis detailed here and on that of Martell and co-workers concerning Cu(II),[7] Cu(II) complex,[8] and VO^{2+} [9]-catalyzed oxidation of ascorbic acid, complex **3** appears to be a reasonable, albeit hypothetical, intermediate in the oxidation of acetol. The salient features of this hypothesis are as follows: (a) Removal of substrate alkoxy proton effectively promotes electron transfer: the anion can be expected to be a better reductant. (b) The electron transferred to metal would go into the $d_{x^2-y^2}$ (or hybrid) orbital; electron transfer to O_2 would be into an antibonding orbital from either a d_{xz} or d_{yz} metal one.[7,35] (c) This latter electron transfer could be catalyzed by proton transfer to the nascient O_2^-; protonation makes O_2^- a poorer reductant, i.e., makes the O_2/O_2^- $E^{\circ\prime}$ less negative.[36] (d) This general acid catalysis is what is observed at low pH in the presence of excess pyridine (β = 0.11). (e) Turnover, i.e., electron transfer, requires a proton transfer (ionization); that is, below pH 4 oxidation requires $pyrH^+$, while above pH 5 Brønsted-catalysis involves H^+-transfer from –OH to pyridine or simple group ionization. Proton transfer to the nascient O_2^- from H_2O also may be catalytic in this pH region. (f) The reorganization of the coordination sphere to square pyramidal (or a distorted octahedron) promotes the axial π-bonding of molecular oxygen.[30] (g) $HO_2^\bullet$ does not dissociate, but is reduced to H_2O_2 via a second electron transfer within this complex. Irrespective of the validity of the interpretation of the results, they indicate clearly that an understanding of this structurally simple system should be invaluable in the elucidation of mechanisms of O_2 activation by related metal centers. This understanding remains the focus of our work.

Acknowledgment. We acknowledge Dr. Eric Dahmer for his assistance in the use of PENNZYME and Angela Grys and Gloria Viola for the preparation of this manuscript. The financial support of the National Science Foundation (DMB 8417792) is greatly appreciated.

Registry No. D_2, 7782-39-0; acetol, 116-09-6; copper(II) tetrapyridine, 36210-39-6; galactose oxidase, 9028-79-9.

(31) Barron, E. S. G.; De Meio, R.; Klemperer, F. W. *J. Biol. Chem.* **1936**, *112*, 625–640.
(32) Weissberger, A.; Luvalle, J. E.; Thomas, D. S., Jr. *J. Am. Chem. Soc.* **1943**, *65*, 1934–1939.
(33) George, P. *J. Chem. Soc.* **1954**, 4349–4359.
(34) Beck, M. T.; Gorog, S. *Acta Chim. Acad. Sci. Hung.* **1961**, *29*, 401–408.
(35) Ochiai, E.-I. *Bioinorganic Chemistry*; Allyn and Bacon: Boston, 1977; Chapter 10.
(36) Fee, J. A. In *Oxidases and Related Redox Systems*; King, T. E., Mason, H. S., Morrison, M., Eds.; Pergamon Press: New York, 1982; pp 101–149.